Geophys. J. Int. (2002) **148,** 313–319

Spontaneous polarization of water in porous structure of a solid body

Lech Rusiniak

Institute of Geophysics, Polish Academy of Sciences, ul. Ks. Janusza 64, 01–452 *Warsaw, Poland. E-mail: rusiniak @igf.edu.pl*

Accepted 2001 July 24. Received 2000 December 12; in original form 1998 November 20

SUMMARY

The dielectric permittivity was measured in the frequency range from 5 to 13 MHz for artificial, laboratory-made solid samples of gypsum with different water contents. The measurements were made on distilled water and three samples with different porosity and structure. The two electrode method was used. Two kinds of electrodes were employed, viz. blocking and non-blocking ones. Simple physical models of saturated porous medium in electric field and the equivalent circuits are presented. The dielectric permittivity of water can be estimated from the data by calculations based on the simple model. Two types of dispersion were observed, associated with domain resonance and apparent Debye resonance.

Key words:

1 INTRODUCTION

For a long time, dielectric materials containing water have been an object of interest for both practical and scientific reasons. Such a material is very interesting from physical point of view, as it is a solid dielectric with a liquid dipole dielectric in the pores, cracks and other structural defects. There are good prospects for practical use of the results in non-destructive testing and in the measurement of water inside various products and materials.

In geophysics, electrical properties of rocks, minerals and non-consolidated materials containing water, oil and gas, are subject to laboratory studies as well as field surveys. The fracturing of rocks may generate electromagnetic fields (Nitsan 1977; Ogawa *et al*. 1985; Ogawa 1992; Lockner *et al*. 1986). The knowledge of the conditions under which electromagnetic waves generate and propagate is important. The new sounding instruments measure at very-high and ultra-high radio frequencies the relative dielectric permittivity of a geological formation.

In mines, the impulse radar method is useful for mapping stratigraphic features, detecting and mapping the extent of stress-relief cracks. An estimate of the crack thickness can also be obtained. Suitable monitoring could indicate the rate of growth of a crack and dictate when the remedial action should be taken (Annan *et al*. 1988).

However, neither the results nor their interpretation have been thus far satisfactory. There is a lack of consistent interpretation of the results obtained at low and high frequencies. This follows from the measurement difficulty as well as from the fact that we still do not fully understand the phenomena in question. There is no particular difficulty in measuring the dielectric constant of dry dielectric materials; when precautions are taken to remove all moisture, values of dielectric constant $\varepsilon/\varepsilon_0$ are always quite low, typically 2–15, and show only a slight frequency dependence (Tarkhov 1948; Keller & Licastro 1959; Knight & Nur 1987; Rusiniak 1992, 1994, 1998). Laboratory measurement of dielectric constant of a moist dielectric are difficult to make and have been controversial for some time. In low-frequency (5–10 kHz) measurements of wet materials, very high values of dielectric permittivity have been obtained. These were attributed to measurement errors (Howell & Licastro 1961; Valeev & Parthomenko 1965; Scott *et al*. 1967; Poley *et al*. 1978). It appears that there is no controversy any more, the high ε seems to be accepted.

The interpretation of low and high-frequency measurement (Freedman & Vogiatzis 1979; Sen *et al.* 1981; Lange 1983; Kenyon 1984; Shen *et al*. 1985; Stroud *et al.* 1986; Morimoto & Iwaki 1987; Gosh & Fuchs 1988; Ruffet *et al*. 1991; Haslund 1996) meets difficulties due to the assumption of a constant value of dielectric permittivity of water, $\varepsilon_d = 78$, and the relaxation time, $\tau = 10^{-11}$s (Hasted 1961). The existing theoretical models: Maxwell-Wagner-Silers' (Lysne 1983), Debye's (Debye 1945; Chekowski 1972) and Kirkwood's (1939; 1946) show poor agreement with my experimental data. Many works in this field have been directed to obtaining bounds on dielectric permittivity of a two-component composite (Bergman 1978, 1980, 1982; Milton 1981a,b).

The present work is a continuation of the study using laboratory-made samples of known, homogenous composition. The primary purpose of this paper is to present new experimental data. The second purpose is to show how the data should be interpreted using my new experimental data on distilled water (Rusiniak 2000).

2 PRELIMINARIES

A porous solid body saturated by water is a two-component composite medium, consisting of the solid matrix with complex dielectric constant ε_s^* and water with complex dielectric constant ε_w^*; its the complex dielectric constant ε_c^* satisfies the equation

$$\varepsilon_c^* = \varepsilon_s^* + \varepsilon_w^* \tag{1}$$

We can rewrite this equation in the form:

$$\varepsilon_c^* = \varepsilon_c' + i\varepsilon_c'' = \varepsilon_s' + \varepsilon_D' + i\varepsilon_D'' + \varepsilon_d' + i\varepsilon_d'' + i\,\frac{\sigma}{\varepsilon_0\omega} \tag{2}$$

where ε_D' and ε_D'' are the real and imaginary parts of the dielectric constant of domain structure, ε_d' and ε_d'' are the real and imaginary parts of the dielectric constant of dipole structure, ε_0 is the dielectric constant of free space, σ is the conductance of the sample and ω is the angular frequency. Comparing the left-hand and the right-hand sides of the equation we have

$$\varepsilon_c' = \varepsilon_s' + \varepsilon_D' + \varepsilon_d' \tag{3}$$

$$\varepsilon_c'' = \varepsilon_D'' + \varepsilon_d'' + \frac{\omega}{\varepsilon_0\omega} \tag{4}$$

For a time-varying field, Debye obtained the equations for the real and imaginary parts of the complex dielectric constant:

$$\varepsilon_D' = \varepsilon_\infty + \sum_i \frac{\varepsilon_{Di} - \varepsilon_\infty}{1 + \omega^2\tau_{Di}^2}\,, \tag{5}$$

$$\varepsilon_D'' = \sum_i \frac{\varepsilon_{Di} - \varepsilon_\infty}{1 + \omega^2\tau_{Di}^2}\,\omega\tau_{Di}\,, \tag{6}$$

$$\varepsilon_d' = \varepsilon_\infty + \frac{\varepsilon_d - \varepsilon_\infty}{1 + \omega^2\tau_d^2}\,, \tag{7}$$

$$\varepsilon_d'' = \frac{\varepsilon_d - \varepsilon_\infty}{1 + \omega^2\tau_d^2}\,\omega\tau_d \tag{8}$$

where ε_{Di} and ε_d are the static dielectric constant for domain i and dipole structure, respectively, ε_∞ is the residual dielectric constant for frequencies so high that the domains or the dipoles make no contribution to the dielectric constant, τ_D, τ_d are the relaxation times for domains and dipoles, respectively, $\omega = 2\pi v$ is the angular frequency and v is the frequency.

The relaxation time can be find from the absorption peak

$$\omega_{max}\tau = 1 \tag{9}$$

3 EXPERIMENTAL SET-UP

The measurements was carried out on a Hewlett Packard LF impedance analyser of type HP 4192 A in the frequency range of 5 Hz to 13 MHz. The instrument was working under PC computer control by GPIB. The measurements were made in parallel mode. The two electrode method was used in the present investigations (Scott *et al.* 1967, Knight & Nur 1987). The sample holder was constructed of Plexiglas; it consists of two parts connected by screw junction. Gold plated electrodes with diameters of 43, 40 and 30 mm were used. The measurements were made with blocking electrodes and non-blocking electrodes. The former was covered with a 0.02 mm thick Mylar film. A constant high pressure was applied to the sample-electrode system to eliminate air gaps. The water content was measured by weighting on an analytical balance.

4 SAMPLES

The main objects of our examination were artificial solid samples made from gypsum in the laboratory at various levels of water saturation. Gypsum samples were made from powder in a mould under hydrostatic pressure or without pressure during the bonding process. The samples obtained without pressure have larger porosity. The samples to which pressure was applied in the initial phase have smaller porosity. Samples to which pressure was applied during the binding process have a partially polycrystalline structure. Disk-shaped samples were used with a diameter of 43.6 mm and a height of about 3 mm.

Sample G29 was made with no pressure and had the following parameters: porosity $\Phi = 0.35$, height, $h = 3$ mm, and mass $m_0 = 7.1725$ g. Sample G0T was made under pressure in the initial phase and had: $\Phi = 0.09$, $h = 3.3$ mm, and $m_0 = 10.688$ g. Sample G2.5T was made under pressure $P = 167$ bar and had $\Phi = 0.15$, $h = 2.3$ mm, and $m_0 = 7.506$ g.

Before the measurement, the samples were fully saturated by initially evacuating them in a pressure vessel, and then allowing distilled water to flow into the vessel, thus saturating the sample under atmospheric pressure for some hours. Subsequently, the samples were locked in a measurement chamber. After each measurement the sample was weighed, and then left on a scale to let a certain portion of water evaporate. When the necessary weight was attained, the sample was locked in the measurement chamber again. The samples designated as dry contain trace amounts of water (not measurable on an analitycal balance) due to the interaction with air. Mass of the water in the sample, m, was calculated from

$$m = M - m_0 \tag{10}$$

where m_0 is the mass of the sample before saturation, M is the mass of the sample before each measurement.

5 RESULTS

5.1 Dielectric measurement of distilled water with blocking electrodes

Fig. 1 shows the capacity of dielectric cell filled by distilled water measured at different frequencies with one electrode covered with Mylar foil (1f) and with two electrodes covered with Mylar foil (2f). The obtained curves show strong dispersion near frequencies 30 kHz and 60 kHz, respectively. A similar result was obtained using Mylar foil in the middle of the sample. To explain this effect, Fig. 2 presents the equivalent circuit model representing the measurement cell with the water sample. R1 is the resistance of the water sample, C1 is the capacity associated with dipole dielectric permittivity, and C_s is the series capacity of Mylar foil.

For low frequency we can neglect the capacity C1 and the resistance R1, so the measured effective capacity C_e is:

$$C_{e,\omega\to 0} \approx C_s = S\,\frac{\varepsilon_M\varepsilon_0}{h_M}\,, \tag{11}$$

For high frequency we can neglect the resistance R1 and we have:

$$C_{e,\omega\to\infty} \approx \frac{C_s C_1}{C_s + C_1} = \frac{S\varepsilon_M\varepsilon_d\varepsilon_0}{\varepsilon_M h_w + \varepsilon_d h_M} \tag{12}$$

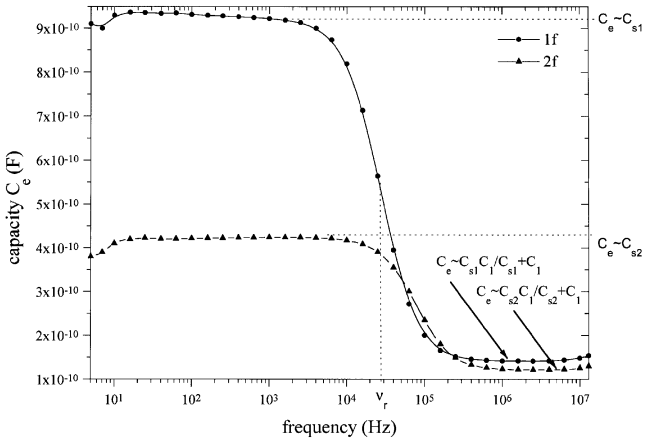

Figure 1. Capacity of measurement cell filled by distilled water, measured at different frequencies with blocking electrodes (thickness $h=2.78$ mm, diameter $d=29$ mm). One electrode is covered by Mylar foil (circles). Two electrodes are covered by Mylar foil (triangles).

where ω is the angular frequency, ε_M is the Mylar dielectric constant, ε_d is the water dipole dielectric constant, ε_0 is the permittivity of free space, h_w is the thickness of water sample, h_M is the thickness of Mylar foil.

The dispersion looks like Debye resonance, so lets us call it an apparent Debye resonance with resonance frequency v_r.

From the condition:

$$R_1 = \frac{1}{\omega_r(C_s + C_1)}, \tag{13}$$

we obtain the expresion for the value of resonance frequency v_r:

$$v_r \approx \frac{1}{2\pi R_1(C_s + C_1)}. \tag{14}$$

5.2 Dielectric measurement of distilled water with non-blocking electrodes

The dielectric permittivity of distilled water was mesured in the frequency range of 5 Hz to 13 MHz with different thicknesses of the sample and for various oscillator levels (Rusiniak 2000). To give an exemple, in Fig. 3 we present the dielectric permittivity

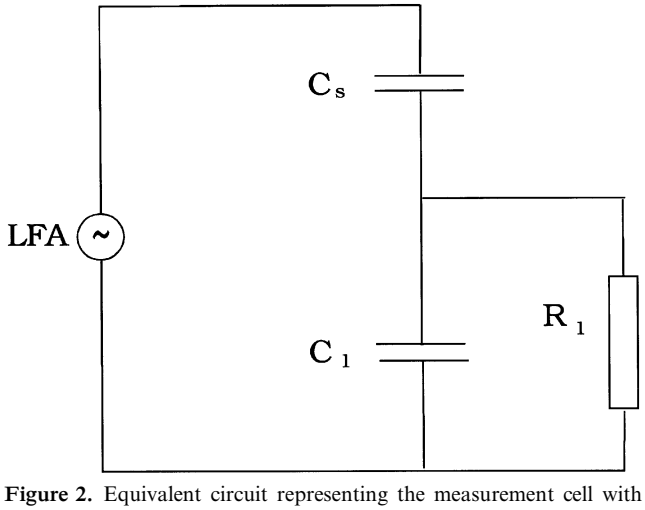

Figure 2. Equivalent circuit representing the measurement cell with blocking electrodes filled by water.

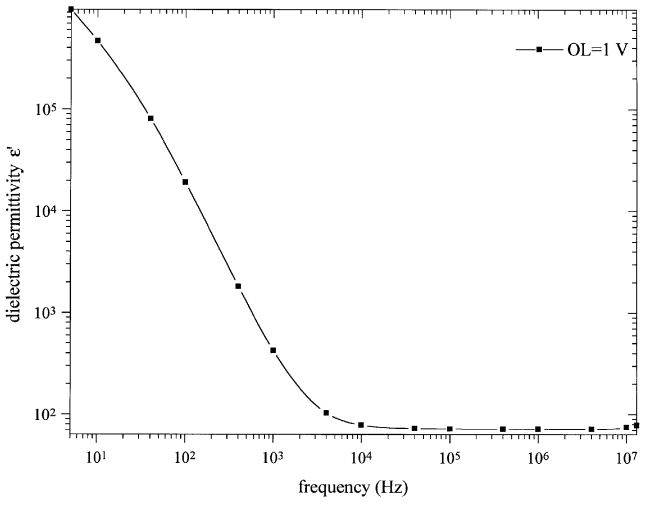

Figure 3. Relative dielectric permittivity of water measured at different frequencies with non-bloking electrodes. Sample with thickness $h=2.78$ mm and diameter $d=29$ mm.

of water measured with non-blocking electrodes. Based on these results, a simple model composed of a dipole liquid with domain structure is described. Possible mechanisms of polarization were shown based on this model. This paper presents conclusions relating to dielectric properties of water which result from the model. A new conductivity model has been proposed for a dipole liquid with domain structure. It was shown that experimental dielectric permittivity curves are a superposition of two Debye curves with different relaxation times and two different values of static dielectric constant. The Debye resonance for lower frequency is associated with oxygen's domain structure and for higher frequency with hydrogen's domain structure.

$$\varepsilon' = \sum_i \varepsilon'_{Di}$$

where ε'_{Di} is the domain dielectric permittivity of domain i.

5.3 Dielectric measurement of water saturated gypsum with blocking electrodes

In Figs 4 and 7 the capacity of water saturated gypsum samples measured with blocking electrodes is plotted against the frequency. As it was shown in Section 5.1, we cannot be simply calculate the dielectric permittivity values from such a measurement. For instance, in Fig. 4 two dispersion areas can be seen for the greatest saturation curve ($m=0.44$ g). To explain this effect, Fig. 5 presents a simple 2-D model of a fully saturated porous sample with blocking electrodes containing one Mylar foil. Rock 1 represents a solid material. Water 1 represents water in long, connected pores and a crack extending from one sample surface to the other. Rock 2 represents a porous material, water 2 represents water in the pores. S1, S_2, S_3 are surface areas.

Fig. 6 shows an equivalent circuit model representing a fully saturated porous sample in the measurement cell with blockig electrodes. C1 repressents the capacity of rock 1, C_{s2} is the capacity of Mylar foil with surface S2, C_2 is the capacity of water 1, R2 is the resistance of water 1, C_{s3} is the capacity of rock 2, C3 is the capacity of water 2, and R_3 is the resistance of water 2.

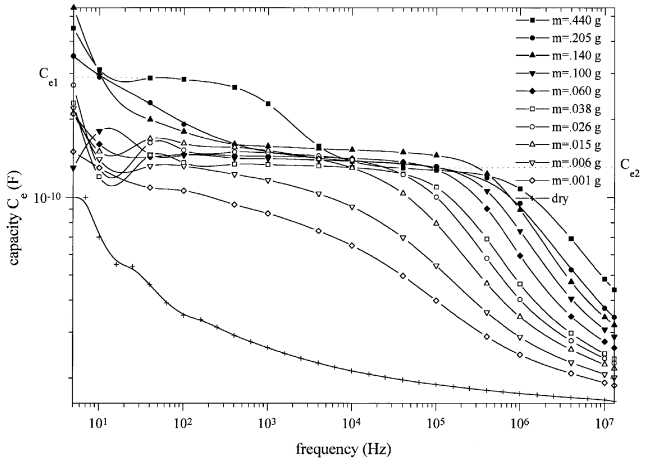

Figure 4. Capacity of measurement cell with gypsum (sample G2.5T) measured with different water contents as a function of frequency with blocking electrodes.

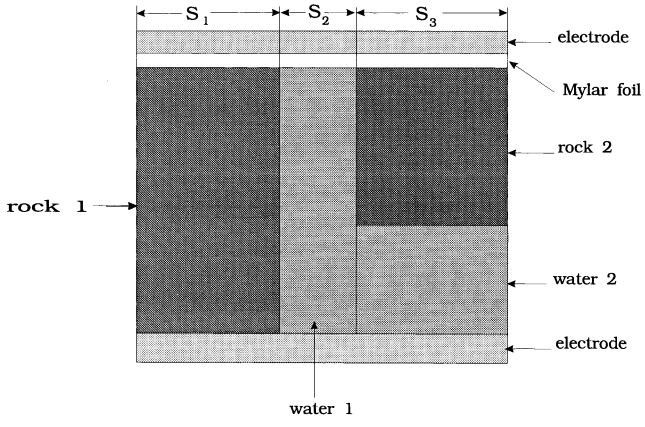

Figure 5. Simple 2-D model of fully saturated porous sample with blocking electrodes.

For full saturation we have the folowing expresions for measured values of effective capacity. For low frequency:

$$C_{e1} = \frac{S_1 \varepsilon_r \varepsilon_0}{h} + \frac{S_2 \varepsilon_M \varepsilon_0}{h_M} + \frac{S_3 \varepsilon_r \varepsilon_0}{h_r} \tag{16}$$

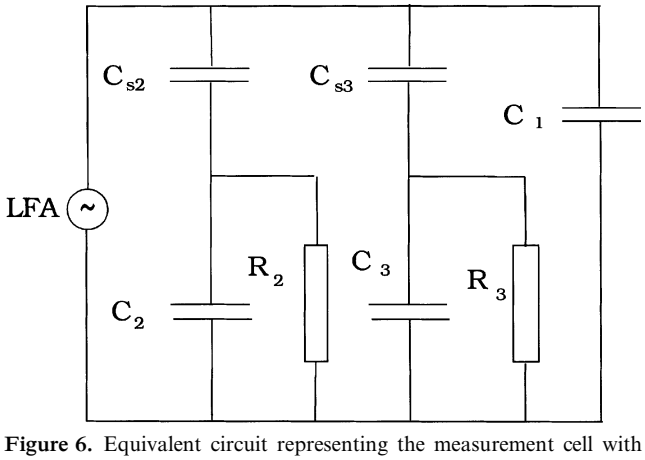

Figure 6. Equivalent circuit representing the measurement cell with blocking electrodes and a saturated porous sample.

For middle frequency, after the first apparent Debye resonance:

$$C_{e2} = \frac{S_1 \varepsilon_r \varepsilon_0}{h} + \frac{S_2 \varepsilon_d \varepsilon_M \varepsilon_0}{\varepsilon_d h_M + \varepsilon_M h} + \frac{S_3 \varepsilon_r \varepsilon_0}{h_r} \tag{17}$$

For high frequency, after the second apparent Debye resonance:

$$C_{e3} = \frac{S_1 \varepsilon_r \varepsilon_0}{h} + \frac{S_2 \varepsilon_d \varepsilon_M \varepsilon_0}{\varepsilon_d h_M + \varepsilon_M h} + \frac{S_3 \varepsilon_d \varepsilon_r \varepsilon_0}{\varepsilon_d h_r + \varepsilon_r h_w} \tag{18}$$

the apparent Debye resonance frequencies are:

$$v_{r1} = \frac{1}{2\pi R_2 (C_{e1} + C_2)} \tag{19}$$

$$v_{r2} = \frac{1}{2\pi R_3 (C_{e2} + C_3)} \tag{20}$$

where $S = S_1 + S_2 + S_3$ is the electrode surface area, $h = h_w + h$ is the sample thickness, h_w is Water 1 thickness, h is Rock 1 thickness, ε_r is relative dielectric constant of rock material, ε_M is the relative dielectric constant of Mylar foil, ε_d is the relative dipole dielectric constant of water, $R1$ is the resistance of Water 1, and R_2 is the resistance of Water 2.

In Fig. 7 the effective capacity of gypsum sample (G29) measured with blocking electrodes is plotted as a function of frequency. Here, the first apparent Debye resonance is masked by domain Debye resonance as a result of slight damage to the Mylar foil.

5.4 Dielectric measurement of water saturated gypsum with non-blocking electrodes

In Fig. 8 the effective capacity of water saturated gypsum sample (G2.5T) measured with non-blocking electrodes is plotted against the frequency. To explain the results, Fig. 9 presents a simple 2-D model of fully saturated porous sample with non-blocking electrodes. Now, we have a mixed case. Measurement was made partly with non-blocking electrodes and partly with blocking electrodes. S2 represents the non-blocking surface electrodes, S3 is the surface electrode which is blocked by Rock 2. Fig. 10 shows the equivalent circuit model representing a fully saturated porous sample in the measurement cell

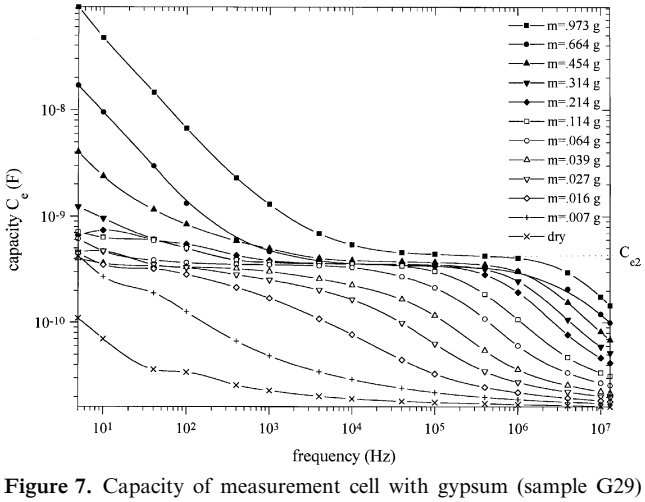

Figure 7. Capacity of measurement cell with gypsum (sample G29) measured with different water contents as a function of frequency (with blocking electrodes).

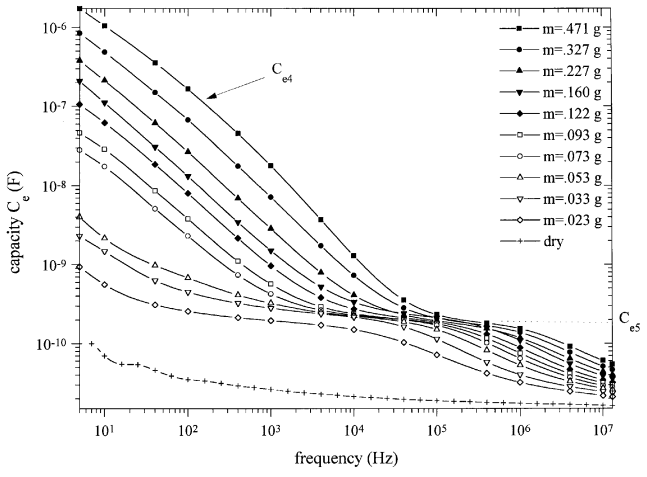

Figure 8. Capacity of measurement cell with gypsum (sample G2.5T) measured with different water contents as a function of frequency (with non-blocking electrodes).

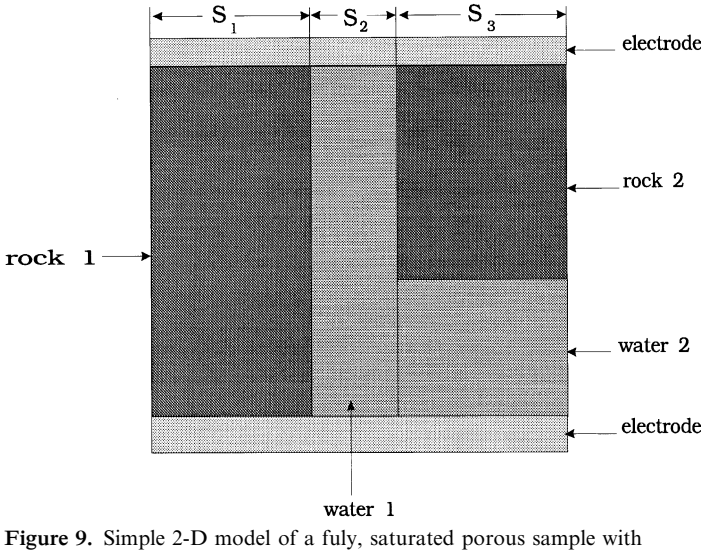

Figure 9. Simple 2-D model of a fuly, saturated porous sample with non-blocking electrodes.

with non-blocking electrodes. For full saturation we have the folowing expresions for the measured values of effective capacity.

For low frequency:

$$C_{e4} = \frac{S_1\varepsilon_r\varepsilon_0}{h} + \frac{S_2\varepsilon'\varepsilon_0}{h} + \frac{S_3\varepsilon_r\varepsilon_0}{h_r} \tag{21}$$

For middle frequency, after domain Debye resonances and before the apparent Debye resonance:

$$C_{e5} = \frac{S_1\varepsilon_r\varepsilon_0}{h} + \frac{S_2\varepsilon_d\varepsilon_0}{h} + \frac{S_3\varepsilon_r\varepsilon_0}{h_r} \tag{22}$$

For high frequency, after the apparent Debye resonance:

$$C_{e6} = \frac{S_1\varepsilon_r\varepsilon_0}{h} + \frac{S_2\varepsilon_d\varepsilon_0}{h} + \frac{S_3\varepsilon_d\varepsilon_r\varepsilon_0}{\varepsilon_d h_r + \varepsilon_r h_w} \tag{23}$$

The apparent Debye resonance frequency is

$$v_r = \frac{1}{2\pi R_1(C_{e5} + C_3)} \tag{24}$$

We have an additional expresion for porosity:

$$\phi = \frac{V_p}{V} = \frac{S_2 h + S_3 h_w}{Sh} \tag{25}$$

where V is the sample volume, V_p is the pore volume, $S = S_1 + S_2 + S_3$, $h = h + h_w$, S is the electrode surface, $S2$ is the non-blocking surface, $S3$ is the blocking surface, h is the sample thickness, h is the average thickness rock 2, and h_w is the average thickness of Water 2.

In Fig. 11 the effective capacity of sample G29 saturated by water measured with non-blocking electrodes is plotted against frequency.

Fig. 12 shows capacity as a function of water content for 5Hz. The linear dependence can be seen in this plot. For small values of saturation we observe a fast increase of capacity, while for greater saturations the increase of capacity is slower. Fig. 13 present the reciprocal relaxation time of apparent Debye resonance as a function of water content for three samples. As can be seen form this figure, the reciprocal relaxation time increases with increasing amount of water in the samples.

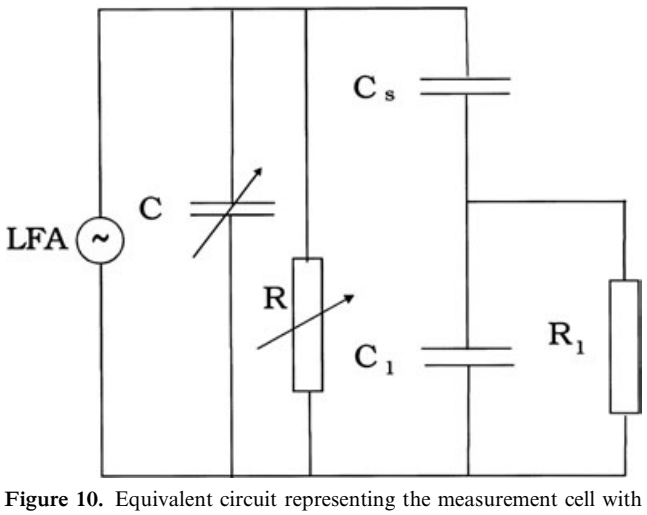

Figure 10. Equivalent circuit representing the measurement cell with non-blocking electrodes and a saturated porous sample.

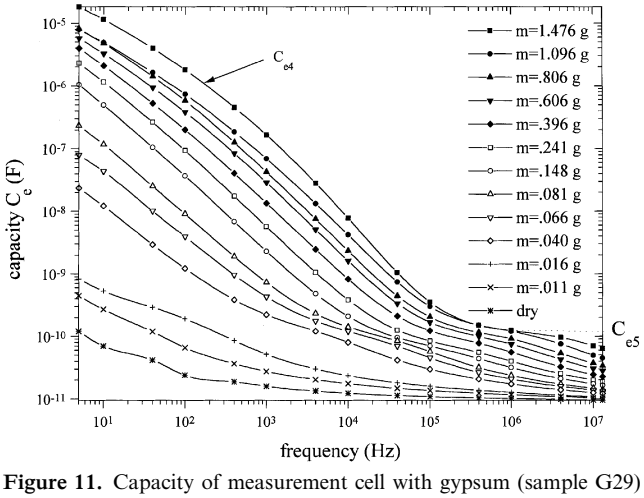

Figure 11. Capacity of measurement cell with gypsum (sample G29) measured with different water contents as a function of frequency (with non-blocking electrodes).

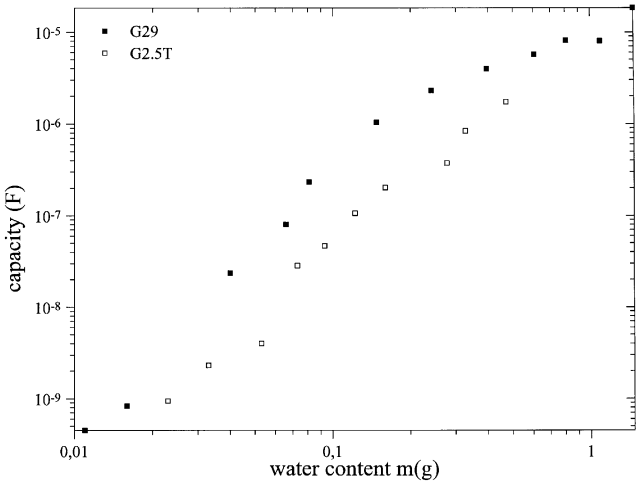

Figure 12. Effective capacity as a function of water content for 5Hz.

6 DISCUSSION

When we compare dispersion curves of clean water (Fig. 3) and water-saturated samples (Figs 7 and 8) we clearly see differences in shape and magnitude. The dispersion curves in rocks are shifted toward higher frequencies. For water-saturated samples we are dealing with a smaller non-blocking area of the electrodes, while the effective dielectric constant is comparable for sample G2.5T and by an order of magnitude greater for sample G29. This may be a result of the rock structure as well as the change in chemical composition of the water. Further detailed studies are indispensible for determining whether the increase in the dispersion curve value results only form the displacement of dispersion curve to higher frequencies and what is the cause of the change in shape. When we reduce the amount of water in the sample, Water 1 and Water 2 can be replaced by air. In the first case this causes a decrease in non-blocking electrode surface and gives rise to an in-series capacitor with a dielectric constant $\varepsilon = 1$. In the other case, an additional in-series capacitor of a dielectric constant $\varepsilon = 1$ is being formed. This leads to a decrease of capacity at lower frequencies as a result of an increase of Water 2 resistance and a small drop of in-series capacitance. The width of apparent resonance may be a measure of inhomogeneity of water saturation in direction perpendicular to the field direction.

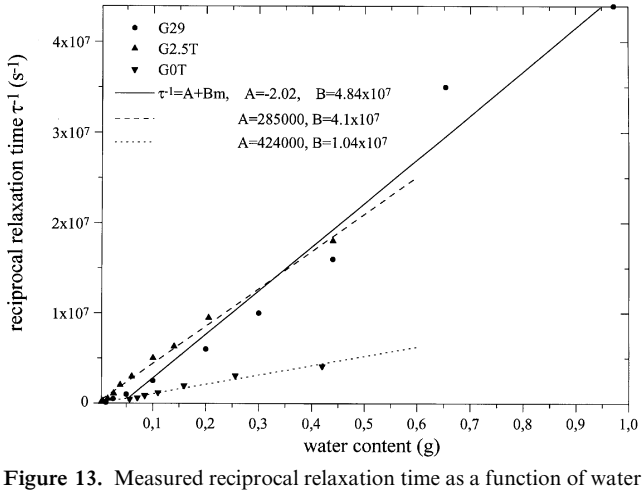

Figure 13. Measured reciprocal relaxation time as a function of water content for three samples

7 CONCLUSIONS

In the electric field, water in solid body defects may behave in two ways: as a liquid of domain structure if the fields are strong (the case of non-blocking electrodes) and as a dipole liquid of dielectric constant $\varepsilon_d = 78$ if the fields are weak (the case of blocking electrodes). Comparing the capacity values for low frequencies for different samples we can draw conclusions about percolational abilities of the material. The differences in dispersion curves obtained for water and water in gypsum may be a consequence of both the chemical composition (water in gypsum contains Ca ions) and the geometry.

ACKNOWLEDGMENTS

The work was partly supported by KBN Grant No.6PO4D03915. I thank J. Kulenkampff for helpful reviews of earlier drafts of this manuscript. I also appreciate suggestions and comments made by an anonymous referee. The author would like to thank A. Dziembowska for her help in the preparation of English version of the manuscript.

REFERENCES

Annan, A.P., Davis, J.L. & Gendzwill, D., 1988. Radar soundig in potash mines, Saskatchewan, Canada, *Geophysics,* **53,** 1556–1564.

Bergman, D.J., 1978. The dielectric constant of a composite material—A problem in classical physics, *Phys. Rept,* **43,** 378–407.

Bergman, D., 1980. J., Exactly solvable microscopic geometries and rigorous bounds for the complex dielectric constant of a two-component composite material, *Phys. Rev. Lett.,* **44,** 1285–1287.

Bergman, D., 1982. J., Rigorous bounds for the complex dielectric constant of a two-component composite, *Ann. Physics,* **138,** 78–114.

Chekowski, A., 1972. *Physics of Dielectrics,* PWN, Warsaw (in Polish).

Debye, P., 1945, .*Polar Molecules,* Dover Publications, New York.

Freedman, R. & Vogiatzis, J.P., 1979. Theory of microwave dielectric constant logging using the electromagnetic wave propagation method, *Geophysics,* **5,** 969–986.

Gosh, K. & Fuchs, R., 1988. Spectral theory for two-component porous media, *Phys. Rev.,* **B38,** 5222–5236.

Haslund, E., 1996. Dielectric dispersion of salt-water-saturated porous glass containing thin glass plates, *Geophysics,* **61,** 2722–2734.

Hasted, J.B., 1961. The dielectric properties of water, in *Progress in Dielectrics,* 3, eds. Birks, J.B. & Hart, J., 101–149, John Wiley and Sons Inc., Chichester.

Keller, G.V. & Licastro, P.H., 1959. Dielectric constant and electrical resistivity of natural-state cores, *USGS Bull.,* **1052-H,** 257–285.

Kenyon, W.E., 1984. Texture effect on megahertz dielectric properties of calcite rock samples, *J. appl. Phys.,* **55,** 3153–3159.

Kirkwood, J.G., 1939. The dielectric polarisation of polar liquids, *J. Chem. Phys.,* **7,** 911–919.

Kirkwood, J.G., 1946. The influence of thindered molecular rotation on the dielectric polarisation of polar liquids, *Trans. Faraday Soc.,* **42A,** 7–13.

Knight, R. & Nur, A., 1987. The dielectric constant of sandstones, 60 kHz to 4 MHz, *Geophysics,* **52,** 644–654.

Lange, J.N., 1983. Microwave properties of saturated reservoirs, *Geophysics,* **48,** 367–375.

Lockner, D.A., Byerlee, J.D., Kuksenko, V.S. & Ponomarev, A.V., 1986. Stick slip, charge separation and decay, *Pure appl. geophys.,* **124,** 601–608.

Lysne, P., 1983. C., A model for the high-frequency electrical response of wet rocks, *Geophysics,* **48,** 6775–6786.

Milton, G.W., 1981a. Bounds on the complex permittivity of a two-component composite material, *J. appl. Phys.,* **52,** 5286–5293.

Milton, G.W., 1981b. Bounds on the electromagnetic, elastic, and other properties of two-component composites, *Phys. Rev. Lett.,* **46,** 542–545.

Morimoto, T. & Iwaki, T., 1987. Dielectric behaviour of adsorbed water, *J. Chem. Soc., Faraday Trans.,* **1,** 83 943–83 956.

Nitsan, U., 1977. Electromagnetic emission accompanying fracture of quartz-bearing rocks, *Geophys., Res. Lett.,* **4,** 333–336.

Ogawa, T., 1992. ELF and VLF radio emissions from rocks, *Res. Lett. Atmos. Electr.,* **12,** 275–281.

Ogawa, T., Oike, K. & Miura, T., 1985. Electromagnetic radiations from, rocks, *J. Geophys. Res.,* **90,** 6245–6249.

Poley, J.Ph, Notteboom, J.J. & de Waal, P, J., 1978. Use of V.H.F, dielectric measurements for borehole formation analysis, *Log Anal,* **3,** 8–30.

Ruffet, C., Guegen, Y. & Darot, M., 1991. Complex conductivity measurements and fractal nature of porosity, *Geophysics,* **56,** 6758–6768.

Rusiniak, L., 1992. Electric properties of rocks from the Legnica-Gogów copper mining district, *Acta Geophys. Pol.,* **40,** 123–138.

Rusiniak, L., 1994. The effect of water on electrical properties of sedimentary rocks, *Annales Geophysicae* (Suppl, I), **12**, *Part I Solid Earth Geophysics and Natural Hazards, C97.*

Rusiniak, L., 1998. Dielectric constant of water in a porous rock medium, *Phys, Chem, Earth,* **23,** 1133–1139.

Rusiniak, L., 2000. Dielectric properties and structure of water at room temperature, New experimental data in 5 Hz-13 MHz frequency range, *Phys, Chem, Earth,* **25,** 201–207.

Scott, J.H., Carroll, R.D. & Cunningham, D.R., 1967. Dielectric constant and electrical conductivity measurements of moist rock: a new laboratory method, *J. geophys. Res.,* **72,** 5101–5115.

Sen, P.N., Scala, C. & Cohen, M., 1981. H., A self-similar model for sedimentary rocks with application to the dielectric constant of fused glass beds, *Geophysics,* **46,** 781–795.

Shen, L.C., Savre, W.C., Price, J. & Athavale, K., 1985. Dielectric properties of reservoir rocks at ultra-high frequencies, *Geophysics,* **4,** 692–704.

Stroud, D., De Milton, G.W. & B.R., 1986. Analytical model for the dielectric response of brine-saturated rocks *Phys, Rev.,* **B34,** 5145–5153.

Tarkhov, A.G., 1948. Resistivity and dielectric constant of rocks in alternating current fields, *Vses. Nauchn.-Issled. Geol. Inst Materialy Geofiz.,* **12,** 3–42.

Valeev, K.A. & E.L., 1965. Parkhomenko E, L., Electrical properties of rocks in constant and alternating electric fields, *Izv, Phys, Solid Earth, English Transl.,* **12,** 45–52.